ACSNANO

www.acsnano.org

ARTICLE

Graphene-Paper Pressure Sensor for Detecting Human Motions

Lu-Qi Tao,[†,‡] Kun-Ning Zhang,[†,‡] He Tian,[†,‡] Ying Liu,[†,‡] Dan-Yang Wang,[†,‡] Yuan-Quan Chen,[†,‡] Yi Yang,[*,†,‡] and Tian-Ling Ren[*,†,‡,§]

[†]Institute of Microelectronics and [‡]Tsinghua National Laboratory for Information Science and Technology (TNList), Tsinghua University, Beijing 10084, China

[§]State Key Laboratory of Transducer Technology, Chinese Academy of Sciences, Beijing 100190, China

Supporting Information

ABSTRACT: **Pressure sensors should have an excellent sensitivity in the range of 0−20 kPa when applied in wearable applications. Traditional pressure sensors cannot achieve both a high sensitivity and a large working range simultaneously, which results in their limited applications in wearable fields. There is an urgent need to develop a pressure sensor to make a breakthrough in both sensitivity and working range. In this paper, a graphene-paper pressure sensor that shows excellent performance in the range of 0−20 kPa is proposed. Compared to most reported graphene pressure sensors, this work realizes the optimization of sensitivity and working range, which is especially suitable for wearable applications. We also demonstrate that the pressure sensor can be applied in pulse detection, respiratory detection, voice recognition, as well as various intense motion detections. This graphene-paper pressure sensor will have great potentials for smart wearable devices to achieve health monitoring and motion detection.**

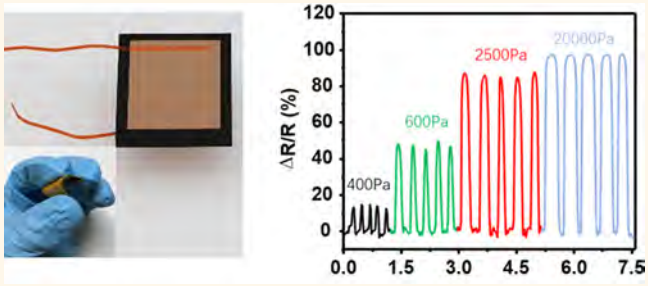

KEYWORDS: *graphene, pressure sensor, paper-based sensor, thermal reduction, human motions*

In recent years, as the application of pressure sensors in wearable devices and electronic skins becomes more and more widespread,[1−5] the development of flexible pressure sensors has attracted a lot of researchers' interests due to their flexibility, light weight, easy processing, low cost, and so on.[6−8] Since the past few years, various materials have been chosen to realize the optimized performance of the pressure sensors. Some researchers have demonstrated that polymers incorporated with carbon nanotubes (CNTs),[9−14] graphene nanosheets,[15] gold nanowires,[16] metal nanoparticles,[17−19] and graphite particles[20] show significant piezoresistive performance. In addition, conductive porous sponges or foams,[21−23] silk,[24] *etc.*, which are combined with graphene or CNTs, can also be considered excellent alternative materials for pressure sensors. Although the structures and the sensing materials of these sensors are different, the sensing mechanism is similar. The contact area of the sensing material will change when pressure is applied, which will result in the change of the electrical property. Pan *et al.* achieved a particularly high sensitivity of 133.1 kPa^{-1} with a pressure sensor based on an elastic microstructured thin polypyrrole film.[25] Tian *et al.* realized a pressure sensor with a large working range of 113 kPa based on face-to-face foam-like laser-scribed graphene.[26] Ge *et al.* studied the graphene pressure sensor with polyurethane (PU) sponge as the substrate, and the sensitivity reached 0.26 and 0.03 kPa^{-1} in the range of 0−3 and 3−10 kPa, respectively.[21] The air gap (porous structure) is a key part for these sensors, which can greatly improve the performance of the pressure sensor. However, the design of an air gap still relies on a complicated fabrication process, which will increase the fabrication cost and sample-to-sample variation. A pressure sensor with excellent performance should possess a large pressure range, a high sensitivity, a long durability, and a good repeatability. However, a problem reveals from the above pressure sensors that a sensor with a large pressure range usually has a poor sensitivity, so the weak pressure cannot be detected. When the sensor has a high sensitivity, it can only measure the pressure under a very small range. This situation limits their applications to a large extent. When a person walks, his pressure on the ground is less than 20 kPa. Therefore, it is of great necessity to develop such kinds of pressure sensors that possess a high sensitivity and a large range (up to 20 kPa) at the same time to expand the application of pressure sensors in smart wearable devices and meet the various demands under different occasions.

Received: April 24, 2017
Accepted: August 11, 2017
Published: August 11, 2017

DOI: 10.1021/acsnano.7b02826
ACS Nano 2017, 11, 8790−8795

Recently, paper-based electronic devices have drawn a wide range of attention in academia for their various advantages that other materials do not have. For instance, they are easily available and renewable at a very low cost.[27,28] In contrast to other substrate materials such as silicon, the fabrication method of paper substrates is much simpler. However, paper also has better mechanical flexibility so it is more appropriate for the fabrication of flexible sensors.[29] With the addition of graphene, carbon nanotubes, or organic materials, the electrical and mechanical properties of paper can be improved greatly, and its application has been expanded greatly. Up to now, a chemical gas sensor which can respond to varying concentration of NH_3[30] and a glucose biosensor for the electrochemical detection of glucose in a two-electrode configuration[31] have been developed. Moreover, various applications utilizing paper such as diodes,[32,33] transistors,[34] energy storage devices,[35−37] antennas,[28] and on-paper electronic circuits[38] have been developed, all of which will be more and more widely employed in the foreseeable future for their excellent performance. In view of the porous structure and good elasticity of paper, it is expected to be a good alternative to improve the performance of the pressure sensor. However, paper-based pressure sensors with high performance are rarely studied. Therefore, our high-performance pressure sensor based on paper substrate is of great research value in artificial skins and wearable electronic devices.

In this paper, we propose a paper-based high-performance pressure sensor. We mix the tissue paper with the graphene oxide (GO) solution to obtain a GO paper. The GO paper can be reduced in the drying oven for several hours of heat. This method not only can improve the electrical conductivity significantly but also is simple and easy to operate, which shows a great potential for large-scale production of graphene materials. We explore the number of layers of tissue paper's effect on the sensitivity of the pressure sensor. The testing results show that the performance of the pressure sensor based on tissue paper has been improved greatly with pressure ranges from 0 to 20 kPa and a sensitivity of up to 17.2 kPa^{-1}. Moreover, the paper-based pressure sensor can realize the measurement of wrist pulse, speaking, breathing, and motion states. Compared to the mentioned pressure sensors researched previously, it has obvious advantages in achieving an ultrahigh sensitivity within an enough working range that can better meet the requirements in detection of human physiological activities. Therefore, the paper-based pressure sensor will have great potential in the field of smart skin, healthcare, and wearable devices.

RESULTS AND DISCUSSION

The fabrication process is demonstrated in Figure 1a. We cut the tissue paper into squares and leave them to soak in the GO solution. Then with thermal reduction method, the samples are transformed into reduced GO (rGO) paper. Finally, after electrode connection and encapsulation, the graphene pressure sensors with paper substrate are obtained. Figure 1b,c shows the photos of the pressure sensor, and it shows an excellent flexibility.

The optical image of reduced GO paper is shown in Figure 2a, and the porous structure of paper can be obviously observed. For further analysis of the structure and surface topography of the pressure sensors, we perform scanning electron microscopy (SEM) at different magnifications. The SEM photos are shown in Figure 2b−d. It can be noticed that

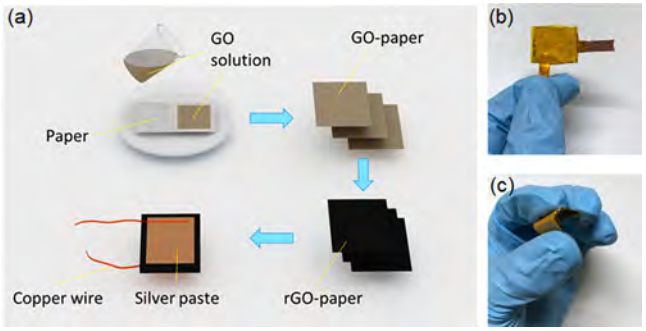

Figure 1. (a) Process of the graphene-based pressure sensors with paper substrate. (b) Photo of pressure sensor encapsulated with PI. (c) Bent sensor showing good flexibility.

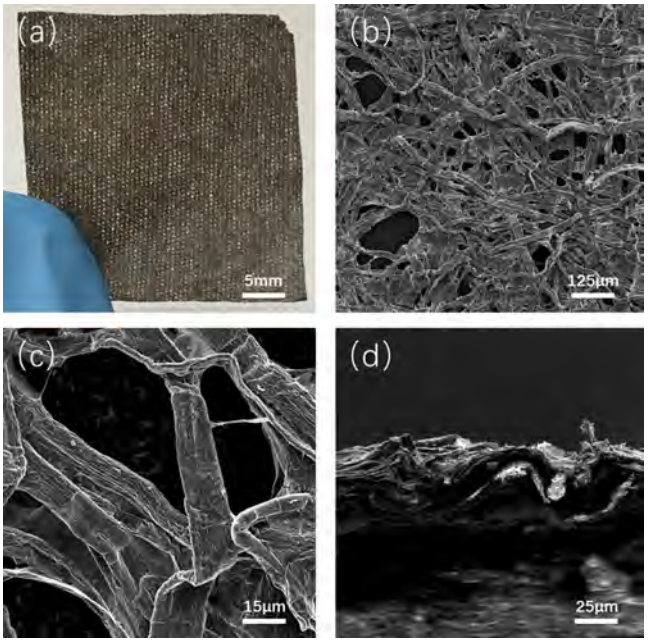

Figure 2. (a) Tissue paper with rGO. (b) SEM photo of the tissue paper sensor at low magnification. (c) SEM photo of the tissue paper sensor at high magnification. (d) Cross-section photo of the tissue paper sensor.

the paper fibers are overlapped together, and the paper is full of obvious holes. In addition, we can see that the tissue paper is corrugated, and there are many folds and collapses from the cross-section image.

To evaluate the performance of the pressure sensors, we set up an experimental testing platform composed of a Shimadzu AGS-X and Keithley 2400 universal testing machine. The measurement results are as follows in Figure 3. The calculation of sensitivity is based on the formula $S = (\Delta(\delta R)/\delta R)/\Delta P$, where $\delta R = \Delta R/R$, which refers to the relative resistance change, and ΔP refers to the change of pressure. The sensitivity is defined as S_1 in the small pressure range (0 to 2 kPa) and S_2 in the large pressure range (2 to 20 kPa). From Figure 3a, we can see that the tissue paper pressure sensors have a very high sensitivity, and with the increase of pressure, their sensitivity will gradually decline. There are significant differences in the performance with different layers. As the number of layers increases, the sensitivity will rise in the small range and fall in the large range. So the sensitivity of the eight-layer sensor is highest with the value 17.2 kPa^{-1} in the range of 0−2 kPa, and

DOI: 10.1021/acsnano.7b02826
ACS Nano 2017, 11, 8790−8795

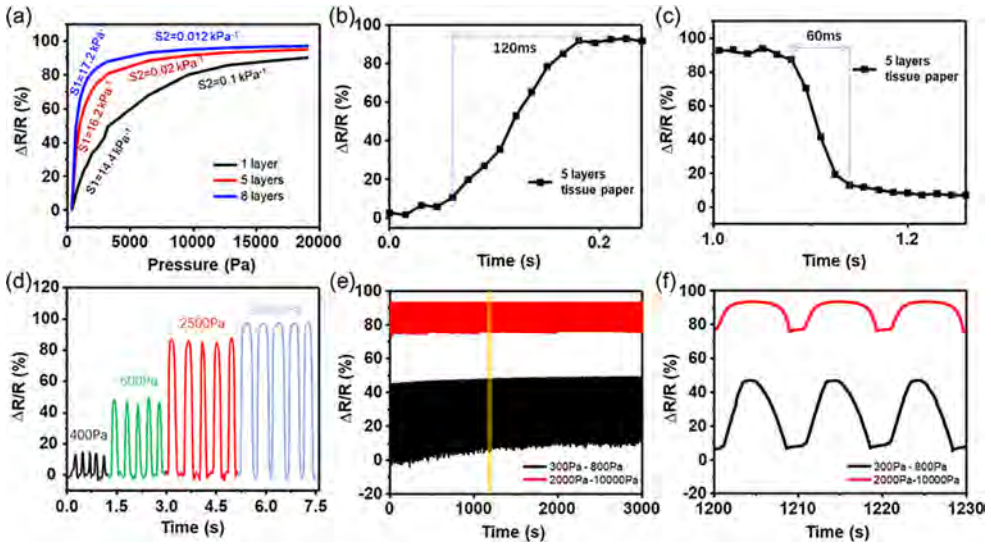

Figure 3. (a) Change of resistance with pressure increases for graphene-based sensor with one, five, and eight layers of tissue paper. (b) Response time of tissue paper pressure sensor. (c) Recovery time of tissue paper pressure sensor. (d) Response test of graphene pressure sensor at different pressure. (e) Test of repeatability characteristics of 300 cycles. (f) Enlarged image of (e).

the one-layer sensor is highest in the range of 2−20 kPa with the value 0.1 kPa^{-1}. The sensitivity of the five-layer sensor in these two ranges, respectively, is 16.2 and 0.02 kPa^{-1}. Compared to the performances of the pressure sensors previously researched that are listed in Table S1, it can be found that the tissue paper sensor achieves an ultrahigh sensitivity in a relatively large range.

The reason for the significant differences in the performance of the different layers of tissue paper pressure sensors is due to the fact that tiny folds on the surface of the paper result in air gaps between layers. The existence of air gaps results in the poor contact between layers, leading to a large origin resistance when no pressure is put on the sensor. Once pressure is applied on the sensor, the air gaps will disappear even if the pressure is very small, and the contact area between paper layers will increase largely. The resistance of the pressure sensor decreases rapidly. Therefore, with the increase of the paper layers, the sensitivity of the pressure sensor in the small pressure range will significantly increase; because the multilayer tissue paper graphene pressure sensor has a very large resistance, the relative resistance change will be less after the air gaps disappear. So, the sensitivity of the multilayer pressure sensor is lower compared to that of the single-layer one in the large pressure range. For the single-layer pressure sensor, its resistance variation relies mainly on the increase in the contact area between the paper fibers. However, when under pressure, the increase in the contact area of the paper fibers is limited; therefore, the sensitivity of single-layer pressure sensors is relatively low.

To further explore different paper substrates and analyze the effects that paper types have on the performances of paper pressure sensors, we also tested the pressure sensors with a filter paper substrate and compared the results with the tissue paper, as shown in Figure S1 in Supporting Information. The sensitivity value of the five-layer filter paper sensor is 7.4 and 0.1 kPa^{-1}. We found that the tissue paper sensors have obviously better performance than filter papers in the small range. The SEM photos in Figure S2 show that the filter paper is quite flat and dense. There are less holes compared with the surface of tissue paper, and the situation is similar in the cross-section photo. From the above analysis, we can deduce that the relative low sensitivity of the filter paper pressure sensor is attributed to the fact that air gaps cannot form between different layers because of its dense structure, strong rigidity, and high flatness of its surface.

With the Sensofar 3D optical profiler, we obtained the 2D view and 3D topography of both pressure sensors from Figure S3. It can be seen from the 3D view that the surface fluctuation range of tissue paper is from −37.5 to 37.5 μm, whereas the range of filter paper is only from −25.9 to 25.9 μm, which indicates that the fluctuation degree of tissue paper is larger and the surface roughness is greater. In the 2D views, the blue zone represents the valley and red zone represents the peak. The 2D view of the tissue paper shows that both the dark blue and dark red areas are larger than the filter paper, which also indicates the difference of structure between these two kinds of paper. The illustration of these photos is consistent with the SEM image results. On the one hand, the tissue paper has a relatively rougher surface; on the other hand, it has a structure with more holes. Therefore, under pressure, the contact area of tissue paper will increase greatly, resulting in the sharper decline of resistance.

Moreover, we also make a measurement of the response time of the two kinds of pressure sensors. The test results are shown in Figure 3b,c and Figure S4. Under the pressure of 20 kPa, the response time and recovery time of the tissue-paper-based pressure sensors are 120 and 60 ms, and the filter-paper-based ones are 75 and 45 ms. The response speed of the filter paper sensor is enhanced about 1/3 compared to that of the tissue paper sensor. So the filter paper pressure sensor is more advantageous when the stress changes rapidly, whereas the tissue paper sensor is more practical to detect weak pressure in consideration of its higher sensitivity.

According to the above analysis, the air gaps between different layers play a key role in maintaining its high sensitivity. In order to research whether the air gaps can stabilize under repeated pressure, it is necessary to test its response and repeatability characteristics. We perform a test on the eight-layer tissue pressure sensor under different pressure values of 400, 600, 2500, and 20000 Pa. The result is shown in Figure 3d.

DOI: 10.1021/acsnano.7b02826
ACS Nano 2017, 11, 8790−8795

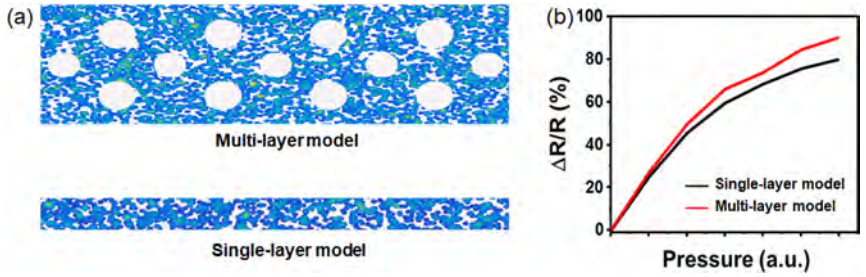

Figure 4. (a) Models of multilayer and single-layer paper-based pressure sensors. (b) Comparison of the simulation results of the multilayer model and single-layer model.

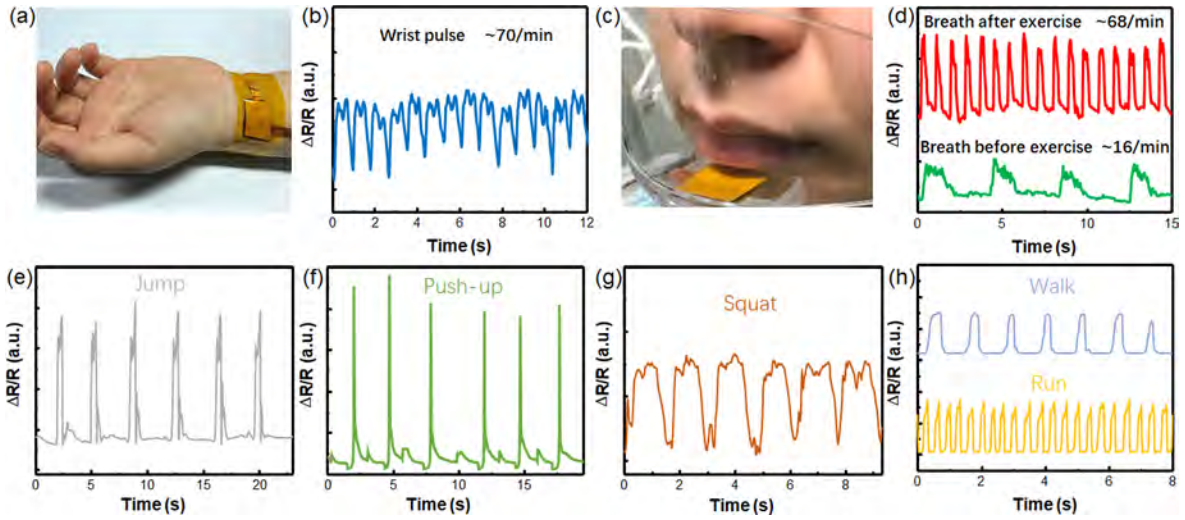

Figure 5. (a) Application for wrist pulse detection. (b) Pulse waveform of the tester. (c) Application for respiration detection. (d) Response curves for breathing before and after exercise. (e–h) Response curves for the tester's movements of jumping, push-ups, squatting, walking, and running in a motion monitoring test.

Under each pressure, the sensor has a good and stable response, and the relative change in resistance of the sensor increases significantly over the small pressure range. Therefore, this kind of graphene pressure sensor is particularly suitable for detection devices where high sensitivity is required. Figure 3e shows the repeatability testing result of tissue paper pressure sensors of 300 cycles under a small range (300–800 Pa) and a large range (2000–10000 Pa). The enlarged view shown in Figure 3f illustrates that the graphene pressure sensor has good reproducibility under both pressure ranges, which means that the air gaps can still exist stably under repeated pressure and do not cause the gradual degradation of the pressure sensor's performance. In addition, we test the sample-to-sample variation, which is shown in Figure S5 in the Supporting Information. The variation will decrease with the increasing pressure. Moreover, the hysteresis of the pressure sensor is also an important characteristic. From Figure S6, we can see that the single-layer sensor has a lower hysteresis compared with that of the multilayer sensor. The hysteresis of the multilayer sensor is mainly caused by the existence of air gaps between graphene paper.

We can see that the sensitivity of the multilayer paper-based graphene pressure sensor is higher than that of the single-layer ones. In order to analyze this phenomenon, we established two randomly distributed models. As shown in Figure 4a, for a single-layer sensor, we use a random distribution model to represent paper fibers. In the simulation, we build a lot of points and the conductivity of each point is σ. When two points are overlapped, the conductivity of the overlapped part is 2σ. When three points are overlapped, the conductivity of the overlapped part is 3σ. The rest can be done in the same manner. When the pressure is applied, the overlapped part will be changed and then the resistance will also be changed. In addition, we increase the thickness of the model to a simulate multilayer sensor and introduce layered white holes in the model to represent the air gaps between different layers. The simulation result shown in Figure 4b means that the sensitivity of the multilayer model is higher than that of the single-layer device. The theoretical results are in agreement with the experimental results. It is proven that the sensitivity can be improved by the existence of air gaps.

In consideration of the high sensitivity, large measuring range, excellent response, and repeatability properties of the pressure sensors we proposed, they can be applied in many fields. Our tests indicate that the pressure sensors can be used either to detect weak stress such as voice recognition, respiration, and wrist pulse or to sense intense exercise. First, as displayed in Figure 5a, the graphene pressure sensor is fixed to the tester's wrist with PI tape, and it has a good response to the pulse beat. We know from the testing curve in Figure 5b that the pulse rate is approximately 70 times/min, which is close to the normal level. The graphene pressure sensor can also be used for the measurement of respiration rate. In Figure 5c, the tester wears a transparent mask with the graphene pressure sensor fixed in it, and the gas pressure produced by each breath will increase the resistance of the pressure sensor.

DOI: 10.1021/acsnano.7b02826
ACS Nano 2017, 11, 8790–8795

The results in Figure 5d demonstrate that the tester's respiration rate is about 16 times/min before exercise and 68 times/min after exercise. The tested rate conforms to the practical level. From a medical point of view, breathing state and pulse rate are important health indicators of the body, which can reflect the health level, especially for some patients suffering from asthma, heart attack, or other diseases. Through the pressure sensor we used, the real-time detection of health status can be achieved, and it can help to monitor some respiratory and heart diseases and is of great significance in the field of wearable medical health.

The graphene pressure sensor is also quite effective for detection of violent pressure changes. The graphene pressure sensor is placed in the tester's soles and palm of the hand, and the motion signals can be tested. Figure 5e–h shows the response curves of the graphene pressure sensor to the tester's movements of jumping, push-ups, squatting, walking, and running. It can be seen that the response waveforms of each motion are characteristic, stable, repetitive, and easy to distinguish. If combined with a machine learning algorithm and other technologies, it will be possible for graphene pressure sensors to achieve gait recognition, motion monitoring, and other functions. They hold great application promise in the fields of medical health, wearable electronic devices, and smart robot development.

Furthermore, as shown in Figure S7, the graphene pressure sensor is applied to the throat of the tester to detect the vibration signal of vocal cords when the tester is speaking. The three figures exhibit the resistance–time curves when saying "graphene", "hello", and "sensor". We can see that the curves corresponding to different words are apparently distinct from each other. There are more obvious differences in the details of the curves compared with other pressure sensors researched before, so we expect to achieve more accurate voice recognition. In addition, with each word pronounced four times, the response curve of the pressure sensor is basically the same. We can draw a conclusion that the repeatability is pretty good.

CONCLUSION

In conclusion, the graphene-paper pressure sensor we proposed in this paper demonstrates both excellent sensitivity and large working range. The pressure sensor has significant performance with the pressure range of 20 kPa and ultrahigh sensitivity of 17.2 kPa^{-1} (0–2 kPa). It also shows stable properties. The application tests of the sensor demonstrate that it can be used in respiration and wrist pulse detection, movement monitoring, and voice recognition. Moreover, the sensor has the advantages of great flexibility, simple fabrication process, large-scale production, and low cost. It will have great potentials in smart wearable devices in the future.

METHODS

Fabrication of Paper-Based Pressure Sensors. First, the tissue paper is cut into squares and placed in the culture dish. Then the GO solution with the concentration of 2 mg/mL is dropped into the culture dish, and the paper is soaked completely. After that, the culture dish is put into the oven under the high temperature of 250 °C for 5 h so that the GO is reduced into rGO. After that, we remove the rGO papers. Five- and eight-layer rGO papers are stacked to form the multilayer graphene pressure sensor. One-layer rGO paper is used to form the single-layer graphene pressure sensor. Then the top and bottom layers are connected to the copper foil electrode with silver paste. At last, the pressure sensors with different layers are encapsulated by polyimide (PI) tape. With such a simple process, the fabrication of a paper-based graphene pressure sensor is completed.

Characterization and Performance Testing. The morphologies and structures of the LPG were characterized by a Quanta FEG 450 SEM (FEI Inc.). The 3D optical profiler is performed by Sensofar (Sensofar USA, LLC). The loading of tensile strain was performed with a universal testing machine (Shimadzu AGS-X), and the electrical signals of the strain sensors were recorded by a digital source-meter (Keithley 2400).

ASSOCIATED CONTENT

Supporting Information

The Supporting Information is available free of charge on the ACS Publications website at DOI: 10.1021/acsnano.7b02826.

Figures S1–S7 and Table S1 (PDF)

AUTHOR INFORMATION

Corresponding Authors

*E-mail: yiyang@tsinghua.edu.cn.

*E-mail: rentl@tsinghua.edu.cn.

ORCID

Lu-Qi Tao: 0000-0003-2653-2868

He Tian: 0000-0001-7328-2182

Author Contributions

T.-L.R. and L.-Q.T. designed the project. L.-Q.T. and K.-N.Z. prepared the sample and wrote the manuscript. H.T. helped design the experiments. Y.L. and Y.-Q.C helped characterize the samples. D.-Y.W. performed the simulations. Y.Y. and T.-L.R. helped to modify the manuscript.

Notes

The authors declare no competing financial interest.

ACKNOWLEDGMENTS

This work was supported by National Key R&D Program (2016YFA0200400), National Natural Science Foundation (61574083, 61434001), National Basic Research Program (2015CB352101), Special Fund for Agroscientific Research in the Public Interest (201303107) of China, and Research Fund from Beijing Innovation Center for Future Chip. The authors are also thankful for the support of the Independent Research Program (2014Z01006) of Tsinghua University.

REFERENCES

(1) Takei, K.; Takahashi, T.; Ho, J. C.; Ko, H.; Gillies, A. G.; Leu, P. W.; Fearing, R. S.; Javey, A. Nanowire Active-Matrix Circuitry for Low-Voltage Macroscale Artificial Skin. *Nat. Mater.* **2010**, *9*, 821–826.

(2) Dang, Z.-M.; Yuan, J.-K.; Zha, J.-W.; Zhou, T.; Li, S.-T.; Hu, G.-H. Fundamentals, Processes and Applications of High-Permittivity Polymer–Matrix Composites. *Prog. Mater. Sci.* **2012**, *57*, 660–723.

(3) Shin, M. K.; Oh, J.; Lima, M.; Kozlov, M. E.; Kim, S. J.; Baughman, R. H. Elastomeric Conductive Composites Based on Carbon Nanotube Forests. *Adv. Mater.* **2010**, *22*, 2663–2667.

(4) Yamada, T.; Hayamizu, Y.; Yamamoto, Y.; Yomogida, Y.; Izadi-Najafabadi, A.; Futaba, D. N.; Hata, K. A Stretchable Carbon Nanotube Strain Sensor for Human-Motion Detection. *Nat. Nanotechnol.* **2011**, *6*, 296–301.

(5) Wang, Y.; Yang, R.; Shi, Z.; Zhang, L.; Shi, D.; Wang, E.; Zhang, G. Super-Elastic Graphene Ripples for Flexible Strain Sensors. *ACS Nano* **2011**, *5*, 3645–3650.

(6) Zhang, L.; Hou, G.; Wu, Z.; Shanov, V. Recent Advances in Graphene-Based Pressure Sensors. *Nano LIFE* **2016**, *6*, 1642005.

(7) Hou, Y.; Wang, D.; Zhang, X.-M.; Zhao, H.; Zha, J.-W.; Dang, Z.-M. Positive Piezoresistive Behavior of Electrically Conductive Alkyl-

DOI: 10.1021/acsnano.7b02826
ACS Nano 2017, 11, 8790–8795

Functionalized Graphene/Polydimethylsilicone Nanocomposites. *J. Mater. Chem. C* **2013**, *1*, 515−521.
(8) Rinaldi, A.; Tamburrano, A.; Fortunato, M.; Sarto, M. A Flexible and Highly Sensitive Pressure Sensor Based on a PDMS Foam Coated with Graphene Nanoplatelets. *Sensors* **2016**, *16*, 2148.
(9) Jiang, M. J.; Dang, Z. M.; Xu, H. P. Giant Dielectric Constant and Resistance-Pressure Sensitivity in Carbon Nanotubes/Rubber Nanocomposites with Low Percolation Threshold. *Appl. Phys. Lett.* **2007**, *90*, 042914.
(10) Dang, Z.-M.; Jiang, M.-J.; Xie, D.; Yao, S.-H.; Zhang, L.-Q.; Bai, J. Supersensitive Linear Piezoresistive Property in Carbon Nanotubes/Silicone Rubber Nanocomposites. *J. Appl. Phys.* **2008**, *104*, 024114.
(11) Jiang, M.-J.; Dang, Z.-M.; Xu, H.-P.; Yao, S.-H.; Bai, J. Effect of Aspect Ratio of Multiwall Carbon Nanotubes on Resistance-Pressure Sensitivity of Rubber Nanocomposites. *Appl. Phys. Lett.* **2007**, *91*, 072907.
(12) Jiang, M.-J.; Dang, Z.-M.; Xu, H.-P. Significant Temperature and Pressure Sensitivities of Electrical Properties in Chemically Modified Multiwall Carbon Nanotube/Methylvinyl Silicone Rubber Nanocomposites. *Appl. Phys. Lett.* **2006**, *89*, 182902.
(13) Hwang, J.; Jang, J.; Hong, K.; Kim, K. N.; Han, J. H.; Shin, K.; Park, C. E. Poly (3-Hexylthiophene) Wrapped Carbon Nanotube/poly (Dimethylsiloxane) Composites for Use in Finger-Sensing Piezoresistive Pressure Sensors. *Carbon* **2011**, *49*, 106−110.
(14) Jung, S.; Kim, J. H.; Kim, J.; Choi, S.; Lee, J.; Park, I.; Hyeon, T.; Kim, D. Reverse-Micelle-Induced Porous Pressure-Sensitive Rubber for Wearable Human-Machine Interfaces. *Adv. Mater.* **2014**, *26*, 4825−4830.
(15) Chen, L.; Chen, G. H.; Lu, L. Piezoresistive Behavior Study on Finger-Sensing Silicone Rubber/Graphite Nanosheet Nanocomposites. *Adv. Funct. Mater.* **2007**, *17*, 898−904.
(16) Gong, S.; Schwalb, W.; Wang, Y.; Chen, Y.; Tang, Y.; Si, J.; Shirinzadeh, B.; Cheng, W. A Wearable and Highly Sensitive Pressure Sensor with Ultrathin Gold Nanowires. *Nat. Commun.* **2014**, *5*, 3132.
(17) Sangeetha, N. M.; Decorde, N.; Viallet, B.; Viau, G.; Ressier, L. Nanoparticle-Based Strain Gauges Fabricated by Convective Self Assembly: Strain Sensitivity and Hysteresis with Respect to Nanoparticle Sizes. *J. Phys. Chem. C* **2013**, *117*, 1935−1940.
(18) Maheshwari, V.; Saraf, R. F. High-Resolution Thin-Film Device to Sense Texture by Touch. *Science* **2006**, *312*, 1501−1504.
(19) Segev-Bar, M.; Landman, A.; Nir-Shapira, M.; Shuster, G.; Haick, H. Tunable Touch Sensor and Combined Sensing Platform: Toward Nanoparticle-Based Electronic Skin. *ACS Appl. Mater. Interfaces* **2013**, *5*, 5531−5541.
(20) Someya, T.; Sekitani, T.; Iba, S.; Kato, Y.; Kawaguchi, H.; Sakurai, T. A Large-Area, Flexible Pressure Sensor Matrix with Organic Field-Effect Transistors for Artificial Skin Applications. *Proc. Natl. Acad. Sci. U. S. A.* **2004**, *101*, 9966−9970.
(21) Yao, H.; Ge, J.; Wang, C.; Wang, X.; Hu, W.; Zheng, Z.; Ni, Y.; Yu, S. A Flexible and Highly Pressure-Sensitive Graphene−Polyurethane Sponge Based on Fractured Microstructure Design. *Adv. Mater.* **2013**, *25*, 6692−6698.
(22) Han, J.-W.; Kim, B.; Li, J.; Meyyappan, M. Flexible, Compressible, Hydrophobic, Floatable, and Conductive Carbon Nanotube-Polymer Sponge. *Appl. Phys. Lett.* **2013**, *102*, 051903.
(23) Gui, X.; Cao, A.; Wei, J.; Li, H.; Jia, Y.; Li, Z.; Fan, L.; Wang, K.; Zhu, H.; Wu, D. Soft, Highly Conductive Nanotube Sponges and Composites with Controlled Compressibility. *ACS Nano* **2010**, *4*, 2320−2326.
(24) Liu, Y.; Tao, L.-Q.; Wang, D.-Y.; Zhang, T.-Y.; Yang, Y.; Ren, T.-L. Flexible, Highly Sensitive Pressure Sensor with a Wide Range Based on Graphene-Silk Network Structure. *Appl. Phys. Lett.* **2017**, *110*, 123508.
(25) Pan, L.; Chortos, A.; Yu, G.; Wang, Y.; Isaacson, S.; Allen, R.; Shi, Y.; Dauskardt, R.; Bao, Z. An Ultra-Sensitive Resistive Pressure Sensor Based on Hollow-Sphere Microstructure Induced Elasticity in Conducting Polymer Film. *Nat. Commun.* **2014**, *5*, 3002.
(26) Tian, H.; Shu, Y.; Wang, X.-F.; Mohammad, M. A.; Bie, Z.; Xie, Q.-Y.; Li, C.; Mi, W.-T.; Yang, Y.; Ren, T.-L. A Graphene-Based Resistive Pressure Sensor with Record-High Sensitivity in a Wide Pressure Range. *Sci. Rep.* **2015**, *5*, 8603.
(27) Eder, F.; Klauk, H.; Halik, M.; Zschieschang, U.; Schmid, G.; Dehm, C. Organic Electronics on Paper. *Appl. Phys. Lett.* **2004**, *84*, 2673−2675.
(28) Lin, Y.; Gritsenko, D.; Liu, Q.; Lu, X.; Xu, J. Recent Advancements in Functionalized Paper-Based Electronics. *ACS Appl. Mater. Interfaces* **2016**, *8*, 20501−20515.
(29) Russo, A.; Ahn, B. Y.; Adams, J. J.; Duoss, E. B.; Bernhard, J. T.; Lewis, J. A. Pen-on-Paper Flexible Electronics. *Adv. Mater.* **2011**, *23*, 3426−3430.
(30) Mirica, K. A.; Weis, J. G.; Schnorr, J. M.; Esser, B.; Swager, T. M. Mechanical Drawing of Gas Sensors on Paper. *Angew. Chem., Int. Ed.* **2012**, *51*, 10740−10745.
(31) Santhiago, M.; Kubota, L. T. A New Approach for Paper-Based Analytical Devices with Electrochemical Detection Based on Graphite Pencil Electrodes. *Sens. Actuators, B* **2013**, *177*, 224−230.
(32) Zhang, Y.; Ge, L.; Li, M.; Yan, M.; Ge, S.; Yu, J.; Song, X.; Cao, B. Flexible Paper-Based ZnO Nanorod Light-Emitting Diodes Induced Multiplexed Photoelectrochemical Immunoassay. *Chem. Commun.* **2014**, *50*, 1417−1419.
(33) Zhao, R.; Zhang, X.; Xu, J.; Yang, Y.; He, G. Flexible Paper-Based Solid State Ionic Diodes. *RSC Adv.* **2013**, *3*, 23178.
(34) Kurra, N.; Dutta, D.; Kulkarni, G. U. Field Effect Transistors and RC Filters from Pencil-Trace on Paper. *Phys. Chem. Chem. Phys.* **2013**, *15*, 8367−8372.
(35) Liu, H.; Crooks, R. M. Paper-Based Electrochemical Sensing Platform with Integral Battery and Electrochromic Read-Out. *Anal. Chem.* **2012**, *84*, 2528−2532.
(36) Leijonmarck, S.; Cornell, A.; Lindbergh, G.; Wagberg, L. Single-Paper Flexible Li-Ion Battery Cells through a Paper-Making Process Based on Nano-Fibrillated Cellulose. *J. Mater. Chem. A* **2013**, *1*, 4671−4677.
(37) Nguyen, T. H.; Fraiwan, A.; Choi, S. Paper-Based Batteries: A Review. *Biosens. Bioelectron.* **2014**, *54*, 640−649.
(38) Wu, H.; Chiang, S. W.; Lin, W.; Yang, C.; Li, Z.; Liu, J.; Cui, X.; Kang, F.; Wong, C. P. Towards Practical Application of Paper Based Printed Circuits: Capillarity Effectively Enhances Conductivity of The Thermoplastic Electrically Conductive Adhesives. *Sci. Rep.* **2014**, *4*, 6275.

DOI: 10.1021/acsnano.7b02826
ACS Nano 2017, 11, 8790−8795